NIH Public Access
Author Manuscript
J Chem Inf Model. Author manuscript; available in PMC 2011 November 22.

Published in final edited form as:
J Chem Inf Model. 2010 November 22; 50(11): 2019–2028. doi:10.1021/ci1002894.

The Assembly-Inducing Laulimalide/Peloruside A Binding Site on Tubulin: Molecular Modeling and Biochemical Studies with [^{3}H]Peloruside A

Tam Luong Nguyen[†], **Xiaoming Xu**[‡], **Rick Gussio**[§], **Arun K. Ghosh**[‡], and **Ernest Hamel**[‖,*]

[†]Target Structure-Based Drug Discovery Group, SAIC-Frederick, Inc., National Cancer Institute at Frederick, Frederick, Maryland 21702, United States

[‡]Departments of Chemistry and Medicinal Chemistry, Purdue University, West Lafayette, Indiana 47907, United States

[§]Information Technology Branch, Developmental Therapeutics Program, Division of Cancer Treatment and Diagnosis, National Cancer Institute at Frederick, National Institutes of Health, Frederick, Maryland 21702, United States

[‖]Screening Technologies Branch, Developmental Therapeutics Program, Division of Cancer Treatment and Diagnosis, National Cancer Institute at Frederick, National Institutes of Health, Frederick, Maryland 21702, United States

Abstract

We used synthetic peloruside A for the commercial preparation of [^{3}H]peloruside A. The radiolabeled compound bound to preformed tubulin polymer in amounts stoichiometric with the polymer's tubulin content, with an apparent K_d value of 0.35 μM. A less active peloruside A analogue, (11-*R*)-peloruside A and laulimalide acted as competitive inhibitors of the binding of the [^{3}H]peloruside A, with apparent K_i values of 9.3 and 0.25 μM, respectively. Paclitaxel, epothilone B, and discodermolide had essentially no ability to inhibit [^{3}H]peloruside A binding, confirming that these compounds bind to a different site on tubulin polymer. We modeled both laulimalide and peloruside A into the binding site on β-tubulin that was identified by Huzil et al. (*J. Mol. Biol.* 2008, 378, 1016–1030) but our model provides a more reasonable structural basis for the protein–ligand interaction. There is a more complete desolvation of the peloruside A ligand and a greater array of favorable hydrophobic and electrostatic interactions exhibited by peloruside A at its β-tubulin binding site. In addition, the protein architecture in our peloruside A binding model was suitable for binding laulimalide. With the generation of both laulimalide and peloruside A binding models, it was possible to delineate the structural basis for the greater activity of laulimalide relative to peloruside A and to rationalize the known structure–activity relationship data for both compounds.

INTRODUCTION

Induction of microtubule assembly by the plant-derived natural product paclitaxel was reported in 1979.1 For many years only taxoid chemotypes were known to possess this property, and taxoids also caused striking morphological changes in cultured cells. Cellular effects include hyperassembly of tubulin into short, bundled microtubules in interphase cells and aster formation in mitotic cells2 as well as accumulation of cells in mitotic arrest, a

© 2010 American Chemical Society

*Corresponding author. hamele@mail.nih.gov Telephone: (301) 846-1678.

NIH-PA Author Manuscript
NIH-PA Author Manuscript
NIH-PA Author Manuscript

NIH-PA Author Manuscript

NIH-PA Author Manuscript

NIH-PA Author Manuscript

property taxoids share with inhibitors of microtubule assembly. In 1995, epothilones A and B, obtained from a myxobacterium, were reported as the lead compounds of a second chemotype with a paclitaxel-like mechanism of action, including inhibition of the binding of paclitaxel to polymer.3 The epothilone report was followed by the description of many additional active compounds, which, for the most part, were marine natural products. These included the sponge-derived laulimalide.4

Most of the newer compounds appear to bind in the taxoid site of tubulin polymers and competitively inhibit the binding of radiolabeled paclitaxel and the fluorescent taxoid derivative flutax-2 to this site.3,5–9 However, first laulimalide10 and then peloruside A,11 another sponge-derived natural product that induces tubulin hyperassembly,12 were shown to lack the ability to inhibit the binding of taxoids to tubulin polymers. Moreover, microtubules formed in the presence of paclitaxel and either laulimalide10 or peloruside A11 contain near stoichiometric amounts of both paclitaxel and the second drug. No evidence was found for coincorporation of laulimalide and peloruside A.11 In addition, both laulimalide and peloruside A can induce enhanced tubulin assembly in concert with a taxoid-site compound but not with each other.13,14 These data suggest that laulimalide and peloruside A bind at the same site on tubulin.

Recently, we developed an enantioselective synthetic route to peloruside A and structural analogues.15 This enabled us to prepare sufficient peloruside A to undertake preparation of [^{3}H]peloruside A. In this report we describe the binding of the radiolabeled compound to tubulin polymer and the effects of other assembly inducing agents, in particular laulimalide, on the binding reaction. The taxoid site compounds examined had little effect on the binding of [^{3}H]peloruside A to microtubules, while laulimalide was a potent competitive inhibitor. We thus have found additional evidence that laulimalide and peloruside A bind in the same site on tubulin polymers. This finding caused us to explore whether laulimalide could be accommodated in a previously described peloruside A binding site on β-tubulin16 and to refine the binding of peloruside A into this site. Figure 1 presents the structures of laulimalide, peloruside A, and (11-*R*)-peloruside A, an active peloruside A analogue, that we used in some of the studies described here.

MATERIALS AND METHODS

Materials

All programs used in the molecular modeling studies were products of Schrodinger, Inc., except as indicated. Peloruside A15 and laulimalide17 were synthesized as described previously. A portion of the peloruside A was labeled with tritium (1.2 Ci/mmol) and repurified at AmBios Biochemicals. Natural epothilone B and natural discodermolide were generously provided by the Merck Research Laboratories and Harbor Branch Oceanographic Institution, respectively. Paclitaxel and [^{3}H]paclitaxel were provided by the Drug Synthesis and Chemistry Branch of the National Cancer Institute. The synthesis of (11-*R*)-peloruside A was essentially as described for peloruside A.15 The nucleotide 2′,3′-dideoxyguanosine 5′-triphosphate was obtained from GE Biosciences. Bovine brain tubulin and heat-treated microtubule-associated proteins were purified as described previously,18 including gel filtration chromatography of the tubulin to remove unbound guanine nucleotide.19

Molecular Modeling

The work of Huzil et al.,16 using hydrogen–deuterium exchange mass spectrometry, localized a binding site for peloruside A on β-tubulin, and we based our binding models for laulimalide and peloruside A on the site that they proposed. The Maestro 9.0 program was

NIH-PA Author Manuscript

NIH-PA Author Manuscript

NIH-PA Author Manuscript

used to build and visualize these models. Simulations employed the OPLS 2005 force field and a distance-dependent dielectric. The ligand structures were generated using LigPrep and refined using Macromodel. Initial docking poses were generated using the Glide program. The 1JFF αβ-tubulin protein structure20 was optimized for ligand binding and used in docking studies.

First, the 1JFF structure was energy minimized, with the α-subunit removed to increase computational speed. The residues identified by Huzil et al.16 were located on the 1JFF β-tubulin structure, and it was observed that, in the absence of bound peloruside A, the proposed binding site in the 1JFF structure assumed a closed conformation with insufficient molecular volume for binding either laulimalide or peloruside A. An examination of other αβ-tubulin structures in the Protein Database, including the 1TVK structure21 used by Huzil et al.16 in their docking studies, revealed a similar closed laulimalide/peloruside A binding site.

Molecular dynamics simulations were performed for 1 ns at 300 and 1500 K on the 1JFF structure to evaluate the conformational changes that could yield an open conformation for the ligand binding site. Large conformational changes in the H9–H9′ (β294–301) and H10 (β332–349) loops (residue numbering and loop terminology as in ref 20) were essential for opening the binding pocket to accommodate laulimalide or peloruside A. However, these molecular dynamics simulations did not reveal the precise motions required to form the binding pocket.

Modeling this binding pocket into the 1JFF β-tubulin structure was not straightforward because the H9–H9′ and H10 loops occlude the pocket. We therefore used a previously developed molecular modeling protocol for engineering binding pockets.22 The modeling challenge was increased because the bioactive conformations of the two ligands were unknown and required evaluating a large conformational landscape for the de novo complementary matching of the H9–H9′ and H10 loops to the bound ligands.

To start, the molecular structures of laulimalide and peloruside A were subjected to molecular dynamics simulations for 1 ns at 1500 K to study the potential solution behavior of each molecule. During the simulations, at 10 ps increments, the structures of laulimalide and peloruside A were collected from the dynamics trajectory. (Conformations of peloruside A were also evaluated for their consistency with NMR data collected when the compound was bound to microtubules.23 Long-range interproton NOE contacts that significantly contributed to establishing the bioactive conformation of peloruside A were the H2 to H12, H3 to H12, H19B to OMe13, and H14B to H20 contacts. Since inter-proton coupling is detected when proton–proton distances are less than 5 Å, we filtered out conformations in which the above contacts were greater than 5 Å.) Presumably, the bioactive conformations, or reasonable approximations of them, exist in this collection of structures, which were all evaluated for their potential energies and hydropathic qualities. To utilize the most realistic bioactive structures, the best set of five conformations for each molecule with low potential energies and high hydropathic qualities was selected for docking studies and to serve as a template to refine the protein binding site.

The 1JFF β-tubulin structure was prepared for initial docking of laulimalide or peloruside A by removing the H9–H9′and H10 loops. This created an open pocket for ligand binding. Into this site, the 10 selected conformations of laulimalide and peloruside A were docked and refined using the high-precision setting of the Glide program. The docked poses were evaluated for their binding affinities using their calculated Gscores and, additionally, were assessed for the presence of both unfavorable and favorable intermolecular contacts between the hydrophobic groups of the ligand and the protein surface, using the Schrodinger analysis

NIH-PA Author Manuscript

NIH-PA Author Manuscript

NIH-PA Author Manuscript

tools. The binding pose of each molecule with the best Gscore and the most favorable hydrophobic interactions at the protein–ligand interface was selected for further refinement.

Next, the H9–H9′ and H10 loops were sequentially refolded onto either laulimalide or peloruside A. In the β-tubulin conformation from the 1JFF structure, residue 294 of the H9–H9′ loop was first reattached to residue 293. The torsions along the peptide backbone of the H9–H9′ loop were manually adjusted to remove unfavorable contacts with the ligands. The subsequent steps involved iterative cycles of: (1) molecular mechanics simulations in order to determine a low-energy conformation for the loop, (2) hydropathic analysis to determine the quality of the atom-to-atom intra-and intermolecular interactions, and (3) manual adjustment and subsequent use of constrained mechanics simulations to remove unfavorable contacts and optimize interactions. At the end of this process, residue 301 in the H9–H9′ loop was reconnected to residue 302 in β-tubulin and energy optimized. The H10 loop was similarly modeled into the ligandbound β-tubulin structure.

These β-tubulin structures with bound laulimalide or bound peloruside A were further refined to optimize the protein–ligand interactions. The models were subjected to iterative cycles of energy minimization and molecular dynamics of both protein and ligand. To help maintain the integrity of the empirically derived coordinates of the β-tubulin in regions that are distinct from the modeled segments of the laulimalide/peloruside A binding site, it was sometimes necessary to fix either the protein structure or the atoms of ligands in Cartesian space. At the final stage, the laulimalide or peloruside A molecule was separated from the binding pocket and redocked de novo using flexible, high-precision docking with the Glide program. The Gscores obtained from this docking simulation were −10.0 for laulimalide and −8.3 for peloruside A. The peloruside A model was also used to evaluate the docking of (11-*R*)-peloruside A, resulting in a Gscore of −8.1. As a last step, the α-tubulin subunit was returned to the binding models, and the αβ-structures with either bound peloruside A or bound laulimalide were energy refined.

Finally, the docked poses of peloruside A and laulimalide were evaluated for the hydropathic quality of the protein–ligand interactions using the HINT program.24 This program was executed according to the protocol in the Discovery Studio 2.5 program of Accelrys, Inc., using parameters described previously.25 HINT provides intuitively reasonable atom-to-atom interaction models, and it was used with an $\exp(-1r)$ distance dependence for hydropathic constants on atom pair interactions. The HINT program quantifies unfavorable hydrophobic–polar interactions, and this was previously used to provide a structural explanation for the different activities of potent inhibitors and inactive close congeners.25 With the models presented here, the HINT program detected no highly unfavorable hydrophobic–polar interactions with either bound peloruside A or bound laulimalide. The HINT program yielded a favorable total interaction constant of 269 for the peloruside A binding model, and, consistent with the experimental observation that laulimalide is the more active agent, the laulimalide binding model yielded a still more favorable total interaction constant of 538.

Biochemical Methods

Where indicated, tubulin assembly was followed turbidimetrically at 350 nm in a Gilford model 250 spectrophotometer equipped with an electronic temperature controller. Binding of [^{3}H]peloruside A or [^{3}H]paclitaxel to tubulin polymer was measured as described previously, 7 except for two changes. First, 100 μM commercial 2′,3′-dideoxyguanosine 5′-triphosphate, as opposed to 50 μM repurified nucleotide, was used to induce tubulin assembly.26 No difference was observed in the extent of assembly of the tubulin (about 90%). Second, the microtubules with bound drug were isolated by centrifugation in a Beckman TLA 55 rotor for 10 min at 37 °C at 30 000 rpm in a Beckman TLX

NIH-PA Author Manuscript

NIH-PA Author Manuscript

NIH-PA Author Manuscript

miniultracentrifuge. The pellets were dissolved in 8 M urea, and protein content and radiolabel in aliquots of the urea solutions were determined. (Previously, supernatant aliquots were counted to measure, by subtraction, bound [^{3}H]paclitaxel.)

The microtubules were formed in a reaction mixture containing 2.5 μM tubulin and 0.75 M monosodium glutamate (taken from a 2 M solution adjusted to pH 6.6 with HCl). The incubation was for 30 min at 37 °C. After this incubation, 200 μL aliquots of the microtubule mixture were added to each reaction vessel. These vessels were at 37 °C and contained, in 50 μL, 0.75 M monosodium glutamate (pH 6.6), 20% (v/v) dimethyl sulfoxide (the solvent used for all drugs), and, as indicated, [^{3}H]peloruside A or [^{3}H]paclitaxel and a potential inhibitor. The final dimethyl sulfoxide concentration was thus 4%, and the drug concentrations referred to in the table and figure legends are those in the final 250 μL reactions. Incubation continued for another 30 min at 37 °C, at which point the reaction mixtures were centrifuged as described above.

RESULTS AND DISCUSSION

Reduced Assembly Activity of (11-*R*)-Peloruside A

Figure 2 presents a comparison of the assembly activity, as a function of reaction temperature, of peloruside A, laulimalide, paclitaxel, and (11-*R*)-peloruside A. The latter compound, while active, was significantly less so than peloruside A and much less active than laulimalide, which had activity comparable to that of paclitaxel. We therefore concluded that the *S*-configuration at C-11 is important to, but not mandatory, for the activity of peloruside A and that (11-*R*)-peloruside A would likely be a competitive inhibitor of peloruside A binding to microtubules (see below).

Comparison of the Binding of [^{3}H]Peloruside A and [^{3}H]Paclitaxel to Tubulin Polymer

Our initial studies with [^{3}H]peloruside A were to compare its binding to microtubules with the binding of [^{3}H]paclitaxel. In the concentration study presented in Figure 3A, there was little difference between the two compounds, and it appeared that both compounds reached saturation when a stoichiometric amount of drug, relative to tubulin, was bound. These data were subjected to Scatchard analysis (Figure 3B), which confirmed a single binding site. The apparent K_d values obtained from the slopes of the Figure 3B curves were 0.35 μM for peloruside A and 0.24 μM for paclitaxel. This value for peloruside A is almost identical to that reported recently at 35 °C when the compound bound to microtubules was quantitated by high-performance liquid chromatography.27

We next examined inhibitory effects of laulimalide, (11-*R*)-peloruside A, epothilone B, and discodermolide on the binding of [^{3}H]peloruside A and [^{3}H]paclitaxel to tubulin polymer (Table 1). As found in previous studies,28 both epothilone B and discodermolide were strong inhibitors of the binding of [^{3}H]paclitaxel to the microtubules, while laulimalide and (11-*R*)-peloruside A were essentially inactive. In contrast, with [^{3}H]peloruside A, it was epothilone B and discodermolide as well as paclitaxel that had little activity, while (11-*R*)-peloruside A and, especially, laulimalide were inhibitory. A more quantitative comparison of the inhibitory effects of laulimalide and (11-*R*)-peloruside A is shown in Figure 4. In this experiment, the IC_{50} obtained for (11-*R*)-peloruside A was 20 μM, while that for laulimalide was substantially lower, about 1 μM.

We next examined varying concentrations of [^{3}H]peloruside A with varying concentrations of (11-*R*)-peloruside A or laulimalide and analyzed the data by standard kinetic methods.29 Hanes plots of the data obtained with both inhibitors yielded families of parallel curves (Figure 5A, (11-*R*)-peloruside A; Figure 5B, laulimalide), and such families of parallel curves indicate that both compounds are competitive inhibitors of the binding of

NIH-PA Author Manuscript

NIH-PA Author Manuscript

NIH-PA Author Manuscript

[^{3}H]peloruside A to microtubules. Dixon analysis29 of these and comparable data from other experiments yielded apparent K_i values of 9.3 ± 3 μM for (11-*R*)-peloruside A and 0.25 ± 0.08 μM for laulimalide. This difference in K_i values is similar to that in IC_{50} values obtained in the experiment presented in Figure 4.

To summarize the biochemical experiments, there was one binding site for peloruside A per tubulin αβ-dimer in microtubules, and the apparent K_d for peloruside A was 0.35 μM. Based on Hanes analysis, laulimalide was a competitive inhibitor of [^{3}H]peloruside A binding to microtubules (apparent K_i, 0.25 μM), implying that both compounds bind to the same site.

Molecular Modeling

We modeled laulimalide and peloruside A into the β-tubulin region identified by Huzil et al. 16 by hydrogen–deuterium exchange mass spectrometry as a likely binding site for peloruside A. However, the orientation of peloruside A in the binding site proposed by these workers is not ideal. The earlier model showed no hydrogen bonds between peloruside A and β-tubulin and oriented key hydrophobic groups of the ligand toward the solvent. By reorienting peloruside A in the binding site, we were able both to introduce hydrogen bonds between ligand and protein and to pack large hydrophobic motifs, such as the bulky, aliphatic side chain at C-15, into hydrophobic pockets. Our binding mode is therefore more consistent with observations that the hydrophobic effects drives ligand binding.30

Figure 6 provides an overview of peloruside A bound to β-tubulin and shows the relative positions of the laulimalide/peloruside A site, the taxoid site (with bound paclitaxel), and the exchangeable nucleotide site with bound GDP. The paclitaxel and GDP conformations and the locations are identical to those in the 1JFF structure.20 Figures 7 and 8 provide detailed binding poses on β-tubulin of peloruside A and laulimalide, respectively. Figure 9 presents a series of laulimalide analogues whose reduced activity was consistent with the Figure 8 model. Finally, Figure 10 presents a superimposition of laulimalide and peloruside A, from their orientations in the binding pocket. This provides insights into a possible pharmacophore and an additional framework for interpreting future structure–activity findings with these two compounds.

As shown in Figure 7, peloruside A forms two hydrogen bonds to β-tubulin. The C-2 hydroxyl is hydrogen bonded to the Val335 backbone carbonyl oxygen atom. While not depicted in the static binding model of Figure 7, the natural solution dynamics of β-tubulin should also permit the C-2 hydroxyl to interact with the backbone carbonyl oxygen atom of Asn339 to form intermittently an alternate hydrogen-bonding interaction (in the Figure 7 model, the oxygen-oxygen distance between the C-2 hydroxyl and the Asn339 carbonyl is 3.2 Å). The second hydrogen bond between peloruside A and β-tubulin shown in Figure 7 is between the C-24 hydroxyl (O-11) of peloruside A and the Tyr312 backbone NH moiety.

Additionally, there is an intramolecular hydrogen bond within peloruside A formed between the hydroxyl groups at C-9 and C-11. In our proposed model, this bond helps to constrain the conformation of the bound peloruside A and, moreover, positions the two hydroxyl groups in close proximity to the Arg308 guanidine side chain, allowing the two hydroxyl groups to form favorable long-range electrostatic interactions with the guanidine moiety or, potentially, water-mediated hydrogen bonds. The native solution dynamics of the β-tubulin structure may even allow intermittent hydrogen-bond formation between these hydroxyls and the Arg308 guanidine side chain.

Besides its electrostatic interactions with the C-9 and C-11 hydroxyl groups, the side chain of Arg308 provides an important hydrophobic binding surface for peloruside A. The dimethyl-substituted C-10 and the unsubstituted C-12 atoms have close hydrophobic

NIH-PA Author Manuscript

NIH-PA Author Manuscript

NIH-PA Author Manuscript

interactions with the aliphatic components of the Arg308 side chain. Thus, the Arg308 residue plays a dual role in stabilizing the interaction of peloruside A with β-tubulin. Several years ago, in a study of mutations in a β-tubulin gene in human breast cancer, Hasegawa et al.31 identified a potential Arg to Cys mutation at position 308, although there was no information about drug resistance associated with the mutation. Modeling the Arg308Cys mutation into our peloruside A model indicates that this mutation would confer resistance to peloruside A.

While favorable enthalpic interactions (e.g., ion–dipole, dipole–dipole, etc.) provide important stability to the ligand–protein interaction, biochemically feasible ligand–protein structures are more importantly characterized by favorable hydrophobic interactions and by a lack of unfavorable hydrophobic–polar interactions.30 These qualities are especially important when forming de novo models, as described here. Besides the C-10/C-12 interaction with the Arg308 side chain, aromatic residues in β-tubulin provide additional, essential binding surfaces for peloruside A. C-25 forms a favorable hydrophobic interaction with Val335. This methyl group is packed against the valyl side chain. Aromatic β-tubulin residues also provide important hydrophobic interactions with peloruside A. The C-10 methyl groups (C-21 and C-22) are wedged against the Tyr312 side chain. The C-26 methyl group is packed against the side chain of Phe296, the C-23 methyl group interacts with the Tyr342 side chain, and the C-27 methyl interacts with the Arg308 aliphatic side chain.

There are a number of important differences between our binding model for peloruside A and that described by Huzil et al.16 In the latter model, the large hydrophobic groups represented by the C-21 and C-22 methyl groups and the C-15 alkyl side chain (C-16-C-20 and its substituents at C-16 and C-18) are solvent exposed. In contrast, in our binding model, these groups were positioned at the interior of the binding pocket and formed the favorable hydrophobic interactions with β-tubulin described above. Second, in the Huzil et al.16 model, the C-15 side chain that includes the C-24 hydroxyl moiety is docked as the most distal segment of peloruside A from Arg308 and Tyr342. In contrast, in our binding model, the side chain was placed in close proximity to these β-tubulin residues, indicating the different topologies of peloruside A in the two binding models.

Recent work by Pera et al.27 identified binding interactions of peloruside A with microtubules by NMR spectroscopy. These workers found that protons H8 and H17, the protons of the C-3 and C-13 methoxy groups, and those of the C-20-and C-22 methyl groups interact strongly with microtubules. They pointed out that their findings were inconsistent with the binding model of Huzil et al.16 In contrast, our binding model provides a structural basis for this peloruside A binding epitope. H8 is packed against the β-carbon of Phe296. H17 is wedged against the α-carbon of Phe343 and the δ-carbon of Arg311. The C-3 methoxy group is packed against Val351. The C-13 methoxy group is wedged against Tyr342. The C-20 methyl group is packed against Phe343. Finally, the C-22 methyl group is wedged against Pro307 and Tyr312.

Based on the limited structure–activity relationship (SAR) data on peloruside A, the interactions of the C-11 hydroxyl group in the model are consistent with the reduced activity that we observed with (11*R*)-peloruside A. According to its best docked conformation, (11*R*)-peloruside A was unable to form a favorable ion–dipole interaction with the Arg308 guanidine moiety, unlike the natural product. Moreover, it is reasonable to infer that the solution structure of (11*R*)-peloruside would be more disordered and, consequently, carry an increased entropic penalty for ligand binding. These lost interactions due to the epimerization of the C-11 hydroxyl largely account for the less favorable docking score for the 11*R* analogue (−8.1) relative to that of the 11*S* natural product (−8.3).

NIH-PA Author Manuscript

NIH-PA Author Manuscript

NIH-PA Author Manuscript

In addition, peloruside B, which lacks the C-25 methyl group and has a hydroxyl moiety at C-3, is about three-fold less cytotoxic than peloruside A.32 Peloruside B is also less active than peloruside A as an inducer of tubulin assembly (data not presented). In the binding model this is explained by loss of the favorable hydrophobic interaction of the C-3 methoxy group with the side chain of Val335 and its replacement with an unfavorable hydrophobic–polar clash between the polar hydroxyl group and the Val335 side chain.

Finally, Pera et al.27 recently reported that analogues of peloruside A bearing acetyl or chloroacetyl groups on O-11 (at C-24) are unable to interact with microtubules.This finding is consistent with our binding model, since the C-24 hydroxyl group of peloruside A forms a hydrogen bond with the Tyr312 backbone NH group in a confined space in the binding pocket. Addition of a bulky substituent at O-11 would severely disrupt this molecular packing as well as cause the loss of a key protein–ligand hydrogen bond.

Biochemical evidence indicates that laulimalide and peloruside A bind in the same region on tubulin, a conclusion strengthened by the experiments presented here, and laulimalide is the more potent agent.10،11،13،14 We therefore modeled laulimalide into the site described by Huzil et al.,16 as shown in Figure 8. In its binding pose, laulimalide assumes a folded conformation, so that the two pyran rings approach each other, with the closest carbon–carbon distance, 3.7 Å, being between C-7 and C-27. This folded conformation is stabilized by an intramolecular hydrogen bond between the C-15 hydroxyl and the side chain pyran oxygen atom (O-7). In our proposed bound conformation, laulimalide possesses an amphipathic molecular surface that is optimal for ligand binding. On one side of the molecule, the two pyran groups form a hydrophobic surface that is wedged into the hydrophobic interior of the β-tubulin binding pocket model.

In contrast, the polar functionalities on the other side of the molecule, consisting of the macrocyclic ester bond, the epoxide, and the C-20 hydroxyl moiety, are oriented toward the solvent and are close to complementary hydrogen-bond acceptors on the H10 loop of β-tubulin. The ester O-1 oxygen atom of laulimalide is close to the Asn339 side chain NH moiety, the epoxide O-3 oxygen atom to the Tyr342 phenolic hydroxyl group, and the C-20 hydroxyl to the backbone NH groups of Ser341 and Tyr342. The presence of structured water molecules suggests that these residues in the H10 loop can form water-mediated hydrogen bonds to laulimalide. In addition, the inherent conformational flexibility of the H10 loop may allow these residues to form direct hydrogen bonds with laulimalide.

Distal from the solvent front, the binding model shows that laulimalide forms a single hydrogen bond to β-tubulin. The side chain pyran oxygen O-7 atom is hydrogen bonded to the Tyr312 backbone NH moiety. Moreover, the O-7 atom also forms an intramolecular hydrogen bond with the O-4 hydroxyl group. This combination of intra- and intermolecular hydrogen bonds tethers laulimalide to the interior of the binding pocket and, consequently, makes an important contribution to binding affinity.

Nevertheless, the binding affinity of laulimalide for this pocket is largely driven by its hydrophobic interactions with β-tubulin. The side chain pyran group is stacked face-to-face with the Phe343 aromatic ring, and the C-28 methyl group of the pyran ring is wedged between the Phe343 ring and the Ile347 side chain. The second pyran group is favorably packed against the Val335 hydrophobic side chain. Finally, the aromatic side chains of Phe296 and Tyr312 provide favorable binding surfaces for the C-30 methyl and C-29 methylene groups, respectively.

Most of the structure–activity data for laulimalide analogues (see Figure 9 for structural diagrams) was obtained in studies of effects of these compounds on cell growth. In almost all cases, analogues were significantly less active than laulimalide itself, with at least a 10-

NIH-PA Author Manuscript

NIH-PA Author Manuscript

NIH-PA Author Manuscript

fold reduction in activity. In compound **1**, the epoxide is replaced with a *trans*-olefin bond.10,33–36 In the laulimalide binding model of Figure 8, this change would result in loss of a stabilizing hydrogen bond, either direct or water-mediated, between the epoxide and the Tyr342 hydroxyl group. In compound **2**, the C-2/C-3 olefin bond is changed from cis to trans.33,35 This would lead to a major conformational change relative to laulimalide and a loss of affinity for the binding pocket. In compound **3**, the C-30 methyl group is removed.37,38 In the binding model, this causes loss of the favorable hydrophobic interaction with the Phe296 phenyl ring. In compound **4**, a methyl group is introduced at the C-20 hydroxyl moiety.34–36 In the binding model, not only is the hydrogen bond to the Tyr342 backbone NH moiety lost, but this modification also causes a highly unfavorable hydrophobic–polar clash between the new methyl group and the Tyr342 backbone NH moiety. Acetylation (compound **5**) or methylation (compound **6**) of the hydroxyl at C-1535 introduces a highly unfavorable hydrophobic–polar interaction with the peptide bond between Pro307 and Arg308. Replacing the C-2/C-3 *cis*-olefin bond with an alkyne moiety37 (compound **7**) introduces intramolecular strain that is only relieved by displacement of the analogue from the interior of the binding pocket (consistent with the 400-fold reduction in cytotoxicity of **7** relative to laulimalide). Epimerization of the C-15 hydroxyl group35 (compound **8**) results in a highly unfavorable interaction between the inverted hydroxyl group and the side chain pyran oxygen atom O-7 (1.8 Å interoxygen distance in the bound conformation). In compound **9**,39 the epoxide is moved from C-16/C-17 to C-15/C-16, with the concomitant addition of a hydroxyl group at C-17 and loss of the hydroxyl at C-15. The latter change, in particular, makes compound **9** incapable of forming the intramolecular hydrogen bond between the C-15 hydroxyl and the side chain pyran oxygen atom, with a consequent inability of the molecule to form a stable folded conformation essential for binding to tubulin. Elimination of the side chain (compound **10**) or even its modification (such as compounds **11** and **12**) always results in significant loss of cytotoxic activity.37,40 With compound **10**, the loss of the side chain results in loss of a significant hydrophobic motif that increases affinity of laulimalide for the binding pocket. Both compounds **11** and **12**, lacking the side chain pyran ring, are unable to form either the hydrogen bond with Tyr312 or the intramolecular hydrogen bond that stabilizes the bound conformation of laulimalide. Based on their binding models, compound **12**, with a Gscore of −7.2, is predicted to bind to tubulin with somewhat greater affinity than compound **11**, with a Gscore of −7.1. With flexible docking models of the two compounds, there was a further increase in the Gscore of compound **12**, to −7.3, but not of compound **11**. The calculated binding affinities of the two compounds are consistent with the approximately 30-fold greater activity of **12** (20–40-fold less cytotoxic than laulimalide) versus **11** (700–1200-fold less cytotoxic).

The last compound shown in Figure 9 (compound **13**, neolaulimalide) was reported by Gollner et al.41 to have activity both in cells and with tubulin equivalent to that of laulimalide. Neolaulimalide differs from laulimalide in that the macrocycle contains an additional atom as C-20, the original C-20 side chain hydroxyl is at C-19, within the macrocycle, and the side chain is one atom shorter and attached to the macrocycle at the C-20 atom. Docking studies with neolaulimalide indicate that it binds with affinity similar to that of laulimalide. Moreover, in the best docked poses, an additional stabilizing hydrogen bond exists between the C-19 hydroxyl group and the C-1 ester carbonyl moiety.

Finally, Figure 10 presents a superimposition of the binding conformations of peloruside A and laulimalide and shows a strong stereochemical correlation between the two compounds. Of particular note is the overlap in the two major hydrophobic regions of each molecule. For peloruside A, the first hydrophobic region consists of the dimethylated C-10 atom and the adjacent pyran ring with its methoxy substituent at C-7. This corresponds to the smaller hydrophobic moiety in laulimalide, which is composed of the C-29 methylene and the C-30 methyl groups. The second hydrophobic region of peloruside A consists of the methoxy

NIH-PA Author Manuscript

NIH-PA Author Manuscript

NIH-PA Author Manuscript

substituent at C-3 (identified by the C-25 methyl group) and the n-butanol motif of the side chain attached at C-17 (identified by C-20 and C-24). This region mapped onto the two pyran rings of laulimalide: the peloruside A methoxy C-25 corresponds to the laulimalide C-7 atom in the macrocycle pyran moiety, and the peloruside A n-butanol (C20–C24) chain to the laulimalide side chain pyran ring. The polar functionalities of peloruside A and laulimalide also exhibit a strong correlation with each other. The ester groups in the macrocycles of the two compounds occupy similar conformational space (the O-1 and O-2 atoms in each compound). The C-16/C-17 epoxide oxygen of peloruside A maps onto the oxygen atom of the methoxy substituent at C-13 (identified by the C-27 methyl group). Finally, the hydroxyl substituent at C-24 (identified as O-11) in peloruside A is bioisosteric with the side chain pyran oxygen atom (O-7) of laulimalide, since both oxygen atoms form hydrogen bonds to the backbone NH moiety of Tyr312. Based on this superimposition, the first hydrophobic region of peloruside A has a larger hydrophobic content than its second region, while, with laulimalide, the opposite is the case. The binding models indicate that the second region occupies more of the interior pocket in β-tubulin than the first region. Therefore, the model predicts that laulimalide should be more active than peloruside A, consistent with experimental observations and accounting for the better Gscore of laulimalide (−10.0) as compared with peloruside A (−8.3).

In concluding, we should note that after completion of this manuscript Bennett et al.42 reported evidence from hydrogen–deuterium exchange mass spectrometry that laulimalide binds in the same site on microtubules as peloruside A, and they modeled laulimalide into this binding site. These workers also noted that the laulimalide/peloruside A site was on the outside of microtubules, as opposed to the inside location of the taxoid site. As with peloruside A, there are substantial differences between our binding pose of laulimalide and theirs. Bennett et al.42 docked the laulimalide macrocycle distal from Arg308 and Tyr342 and placed the side chain furan group nearest to these two amino acid residues. In our model, the laulimalide macrocycle was positioned on top of the side chain furan, which was buried deep inside the binding pocket, with the macrocycle close to Arg308 and Tyr342. Moreover, as described above, in our binding models the laulimalide macrocycle closely overlaps the peloruside A macrocycle.

SUMMARY

We have shown here that [^{3}H]peloruside A bound to preformed tubulin polymer in amounts stoichiometric with the polymer's tubulin content, with an apparent K_d value of 0.35 μM. A less active peloruside A analogue, (11-*R*)-peloruside A, and laulimalide acted as competitive inhibitors of the binding of the [^{3}H]peloruside A, with apparent K_i values of 9.3 and 0.25 μM, respectively. Paclitaxel, epothilone B, and discodermolide had essentially no ability to inhibit [^{3}H]peloruside A binding since they bind to a different site on tubulin polymer. We modeled both laulimalide and peloruside A into the β-tubulin site identified by Huzil et al.16 as a likely binding pocket for peloruside A. Our models provide a structural basis for the superior activity of laulimalide relative to peloruside A as a ligand for this binding pocket and successfully rationalize the key structure–activity relationship data for both compounds.

Acknowledgments

This project has been funded in part with federal funds from the National Cancer Institute, National Institutes of Health, under contract N01-CO-12400. The content of this publication does not necessarily reflect the views or policies of the Department of Health and Human Services nor does mention of trade names, commercial products, or organizations imply endorsement by the U.S. Government. This research was supported in part by the Developmental Therapeutics Program in the Division of Cancer Treatment and Diagnosis of the National Cancer Institute. This work was also funded in part by the National Institutes of Health (A.K.G., GM53386).

NIH-PA Author Manuscript

NIH-PA Author Manuscript

NIH-PA Author Manuscript

REFERENCES AND NOTES

1. Schiff PB, Fant J, Horwitz SB. Promotion of microtubule assembly in vitro by taxol. Nature (London). 1979; 277:665–667. [PubMed: 423966]
2. Schiff PB, Horwitz SB. Taxol stabilizes microtubules in mouse fibroblast cells. Proc. Natl. Acad. Sci. U.S.A. 1980; 77:1561–1565. [PubMed: 6103535]
3. Bollag DM, McQueney PA, Zhu J, Hensens O, Koupal L, Liesch J, Goetz M, Lazarides E, Woods CM. Epothilones, a new class of microtubule-stabilizing agents with a taxol-like mechanism of action. Cancer Res. 1995; 55:2325–2333. [PubMed: 7757983]
4. Mooberry SL, Tien G, Hernandez AH, Plubrukarn A, Davidson BS. Laulimalide and isolaulimalide, new paclitaxel-like microtubule-stabilizing agents. Cancer Res. 1999; 59:653–660. [PubMed: 9973214]
5. Kowalski RJ, Giannakakou P, Hamel E. Activities of the microtubule-stabilizing agents epothilones A and B with purified tubulin and in cells resistant to paclitaxel (Taxol®). J. Biol. Chem. 1997; 272:2534–2541. [PubMed: 8999970]
6. Kowalski RJ, Giannakakou P, Gunasekera SP, Longley RE, Day BW, Hamel E. The microtubule-stabilizing agent discoder-molide competitively inhibits the binding of paclitaxel (Taxol) to tubulin polymers, enhances tubulin nucleation reactions more potently than paclitaxel, and inhibits the growth of paclitaxel-resistant cells. Mol. Pharmacol. 1997; 52:613–622. [PubMed: 9380024]
7. Hamel E, Sackett DL, Vourloumis D, Nicolaou KC. The coral-derived natural products eleutherobin and sarcodictyins A and B: effects on the assembly of purified tubulin with and without microtubule-associated proteins and binding at the polymer taxoid site. Biochemistry. 1999; 38:5490–5498. [PubMed: 10220336]
8. Buey RM, DÍaz JF, Andreu JM, O'Brate A, Giannakakou P, Nicolaou KC, Sasmal PK, Ritzén A, Namoto K. Interaction of epothilone analogs with the paclitaxel binding site: relationship between binding affinity, microtubule stabilization, and cytotoxicity. Chem. Biol. 2004; 11:225–236. [PubMed: 15123284]
9. Edler MC, Buey RM, Gussio R, Marcus AI, Vanderwal CD, Sorensen EJ, Díaz JF, Giannakakou P, Hamel E. Cyclostreptin (FR182877), an antitumor tubulin polymerizing agent deficient in enhancing tubulin assembly despite high affinity for the taxoid site. Biochemistry. 2005; 44:11525–11538. [PubMed: 16114889]
10. Pryor DE, O'Brate A, Bilcer G, Díaz JF, Wang Y, Wang Y, Kabaki M, Jung MK, Andreu JM, Ghosh AK, Giannakakou P, Hamel E. The microtubule stabilizing agent laulimalide does not bind in the taxoid site, kills cells resistant to paclitaxel and epothilones, and may not require its epoxide moiety for activity. Biochemistry. 2002; 41:9109–9115. [PubMed: 12119025]
11. Gaitanos TN, Buey RM, Díaz JF, Northcote PT, Teesdale-Spittle P, Andreu JM, Miller JH. Peloruside A does not bind to the taxoid site on β-tubulin and retains its activity in multidrug-resistant cell lines. Cancer Res. 2004; 64:5063–5067. [PubMed: 15289305]
12. Hood KA, West LM, Rouwé B, Northcote PT, Berridge MV, Wakefield SJ, Miller JH. Peloruside A, a novel antimitotic agent with paclitaxel-like microtubule-stabilizing activity. Cancer Res. 2002; 62:3356–3360. [PubMed: 12067973]
13. Gapud EJ, Bai R, Ghosh AK, Hamel E. Laulimalide and paclitaxel: a comparison of their effects on tubulin assembly and their synergistic action when present simultaneously. Mol. Pharmacol. 2004; 66:113–121. [PubMed: 15213302]
14. Hamel E, Day BW, Miller JH, Jung MK, Northcote PT, Ghosh AK, Curran DP, Cushman M, Nicolaou KC, Paterson I, Sorensen EJ. Synergistic effects of peloruside A and laulimalide with taxoid site drugs, but not with each other, on tubulin assembly. Mol. Pharmacol. 2006; 70:1555–1564. [PubMed: 16887932]
15. Ghosh AK, Xu X, Kim JH, Xu CX. Enantioselective total synthesis of peloruside A: a potent microtubule stabilizer. Org. Lett. 2008; 10:1001–1004. [PubMed: 18247632]
16. Huzil JT, Chik JK, Slysz GW, Freedman H, Tuszynski J, Taylor RE, Sackett DL, Schriemer DC. A unique mode of microtubule stabilization induced by peloruside A. J. Mol. Biol. 2008; 378:1016–1030. [PubMed: 18405918]

NIH-PA Author Manuscript

NIH-PA Author Manuscript

NIH-PA Author Manuscript

17. Ghosh AK, Wang Y, Kim JT. Total synthesis of microtubule-stabilizing agent (-)-laulimalide. J. Org. Chem. 2001; 66:8973–8982. [PubMed: 11749630]

18. Hamel E, Lin CM. Separation of active tubulin and microtubule-associated proteins by ultracentrifugation and isolation of a component causing the formation of microtubule bundles. Biochemistry. 1984; 23:4173–4184. [PubMed: 6487596]

19. Grover S, Hamel E. The magnesium-GTP interaction in microtubule assembly. Eur. J. Biochem. 1994; 222:163–172. [PubMed: 8200341]

20. Löwe J, Downing KH, Nogales E. Refined structure of αβ-tubulin at 3.5 Å resolution. J. Mol. Biol. 2001; 313:1045–1057. [PubMed: 11700061]

21. Nettles JH, Li H, Cornett B, Krahn JM, Snyder JP, Downing KH. The binding mode of epothilone A on αβ-tubulin by electron crystallography. Science. 2004; 305:866–869. [PubMed: 15297674]

22. Nguyen TL, Gussio R, Smith JA, Lannigan DA, Hecht SM, Scudiero DA, Shoemaker RH, Zaharevitz DW. Homology model of RSK2 N-terminal kinase domain, structure-based identification of novel RSK2 inhibitors, and preliminary common pharmacophore. Bioorg. Med. Chem. 2006; 14:6097–6105. [PubMed: 16723234]

23. Jiménez-Barbero J, Canales A, Northcote PT, Buey RM, Andreu JM, Díaz JF. NMR determination of the bioactive conformation of peloruside A bound to microtubules. J. Am. Chem. Soc. 2006; 128:8757–8765. [PubMed: 16819869]

24. Kellogg GE, Semus SF, Abraham DJ. HINT: a new method of empirical hydrophobic field calculation for CoMFA. J. Comput.-Aided Mol. Des. 1991; 5:545–552. [PubMed: 1818090]

25. Nguyen TL, McGrath C, Hermone AR, Burnett JC, Zaharevitz DW, Day BW, Wipf P, Hamel E, Gussio R. A common pharmacophore for a diverse set of colchicine site inhibitors using a structure-based approach. J. Med. Chem. 2005; 48:6107–6116. [PubMed: 16162011]

26. Hamel E, Lustbader J, Lin CM. Deoxyguanosine nucleotide analogues: potent stimulators of microtubule nucleation with reduced affinity for the exchangeable nucleotide site of tubulin. Biochemistry. 1984; 23:5314–5325. [PubMed: 6509023]

27. Pera B, Razzak M, Trigili C, Pineda O, Canales A, Buey RM, Jiménez-Barbero J, Northcote P, Paterson I, Barasoain I, Díaz JF. Molecular recognition of peloruside A by microtubules: the C24 primary alcohol is essential for biological activity. ChemBioChem. 2010; 11:1669–1678. [PubMed: 20665616]

28. Buey RM, Calvo E, Barasoain I, Pineda O, Edler MC, Matesanz R, Cerezo G, Vanderwal CD, Day BW, Sorensen EJ, López JA, Andreu JM, Hamel E, Díaz JF. Cyclostreptin binds covalently to microtubule pores and lumenal taxoid binding sites. Nat. Chem. Biol. 2007; 3:117–125. [PubMed: 17206139]

29. Dixon, M.; Webb, EC.; Thorne, CJR.; Tipton, KF. Enzymes. 3rd. New York: Academic Press; 1979. p. 332-354.

30. Sturtevant JM. Heat capacity and entropy changes in processes involving proteins. Proc. Natl. Acad. Sci. U.S.A. 1977; 74:2236–2240. [PubMed: 196283]

31. Hasegawa S, Miyoshi Y, Egawa C, Ishitobi M, Tamaki Y, Monden M, Noguchi S. Mutational analysis of the class I β-tubulin gene in human breast cancer. Int. J. Cancer. 2002; 101:46–51. [PubMed: 12209587]

32. Singh AJ, Xu C-X, Xu X, West LM, Wilmes A, Chan A, Hamel E, Miller JH, Northcote PT, Ghosh AK. Peloruside, B, a potent antitumor macrolide from the New Zealand marine sponge *Mycale hentscheli*: isolation, structure, total synthesis, and bioactivity. J. Org. Chem. 2010; 75:2–10. [PubMed: 19957922]

33. Ahmed A, Hoegenauer EK, Enev VAS, Hanbauer M, Kaehlig H, öhler E, Mulzer J. Total synthesis of the microtubule stabilizing antitumor agent laulimalide and some nonnatural analogues: the power of Sharpless' asymmetric epoxidation. J. Org. Chem. 2003; 68:3026–3042. [PubMed: 12688769]

34. Wender PA, Hegde SG, Hubbard RD, Zhang L, Mooberry SL. Synthesis and biological evaluation of (-)-laulimalide analogues. Org. Lett. 2003; 5:3507–3509. [PubMed: 12967311]

35. Gallagher JBM, Fang FG, Johannes CW, Pesant M, Tremblay MR, Zhao H, Akasaka K, Li X, Liu J, Littlefield BA. Synthesis and biological evaluation of (-)-laulimalide analogues. Bioorg. Med. Chem. Lett. 2004; 14:575–579. [PubMed: 14741246]

NIH-PA Author Manuscript

NIH-PA Author Manuscript

NIH-PA Author Manuscript

36. Mooberry SL, Randall-Hlubek DA, Leal RM, Hegde SG, Hubbard RD, Zhang L, Wender PA. Microtubule-stabilizing agents based on designed laulimalide analogues. Proc. Natl. Acad. Sci. U.S.A. 2004; 101:8803–8808. [PubMed: 15161976]

37. Paterson I, Menche D, Håkansson AE, Longstaff A, Wong D, Barasoain I, Buey RM, Díaz JF. Design, synthesis and biological evaluation of novel, simplified analogues of laulimalide: modification of the side chain. Bioorg. Med. Chem. Lett. 2005; 15:2243–2247. [PubMed: 15837302]

38. Wender PA, Hilinski MK, Soldermann N, Mooberry SL. Total synthesis and biological evaluation of 11-desmethyllaulimalide, a highly potent simplified laulimalide analogue. Org. Lett. 2006; 8:1507–1510. [PubMed: 16562928]

39. Trost BM, Amans D, Seganish WM, Chung CK. Evaluating transition-metal-catalyzed transformations for the synthesis of laulimalide. J. Am. Chem. Soc. 2009; 131:17087-–17089. [PubMed: 19891433]

40. Mooberry SL, Hilinski MK, Clark EA, Wender PA. Function-oriented synthesis: biological evaluation of laulimalide analogues derived from a last step cross metathesis diversification strategy. Mol. Pharmaceut. 2008; 5:829–838.

41. Gollner A, Altmann K-H, Gertsch J, Mulzer J. The laulimalide family: total synthesis and biological evaluation of neolaulimalide, isolaulimalide and a nonnatural analogue. Chem.—Eur. J. 2009; 15:5979–5997.

42. Bennett MJ, Barakat K, Huzil JT, Tuszynski J, Schreimer DC. Discovery and characterization of the laulimalide-microtubule binding mode by mass shift perturbation mapping. Chem. Biol. 2010; 17:725–734. [PubMed: 20659685]

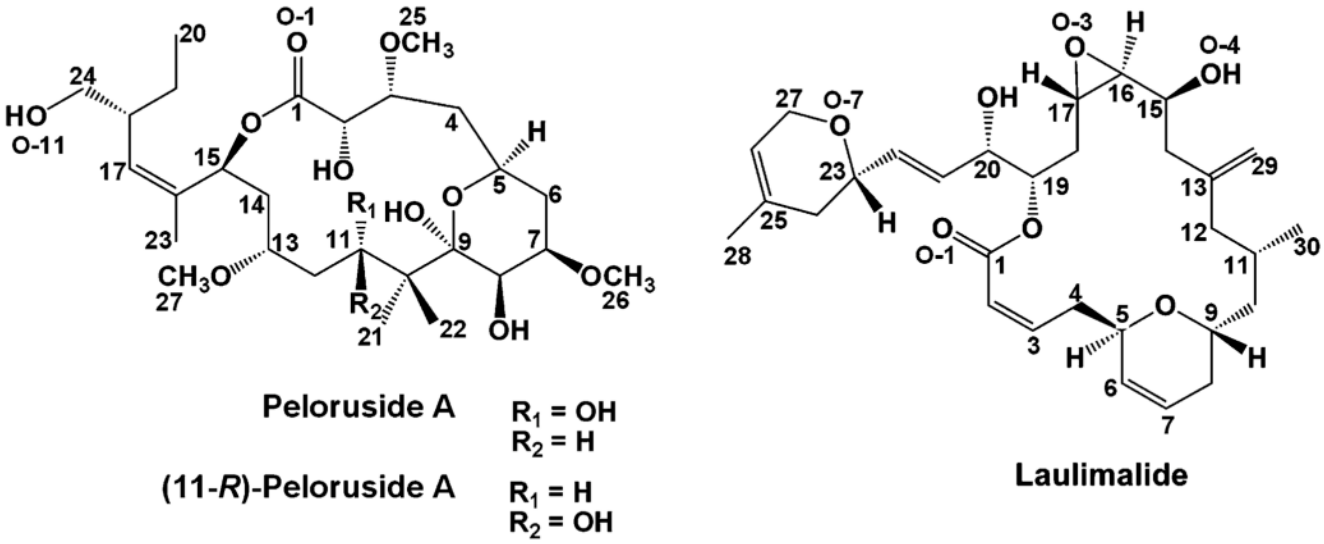

Figure 1.
Molecular structures of peloruside A, (11-*R*)-peloruside A, and laulimalide.

NIH-PA Author Manuscript NIH-PA Author Manuscript NIH-PA Author Manuscript

NIH-PA Author Manuscript

NIH-PA Author Manuscript

NIH-PA Author Manuscript

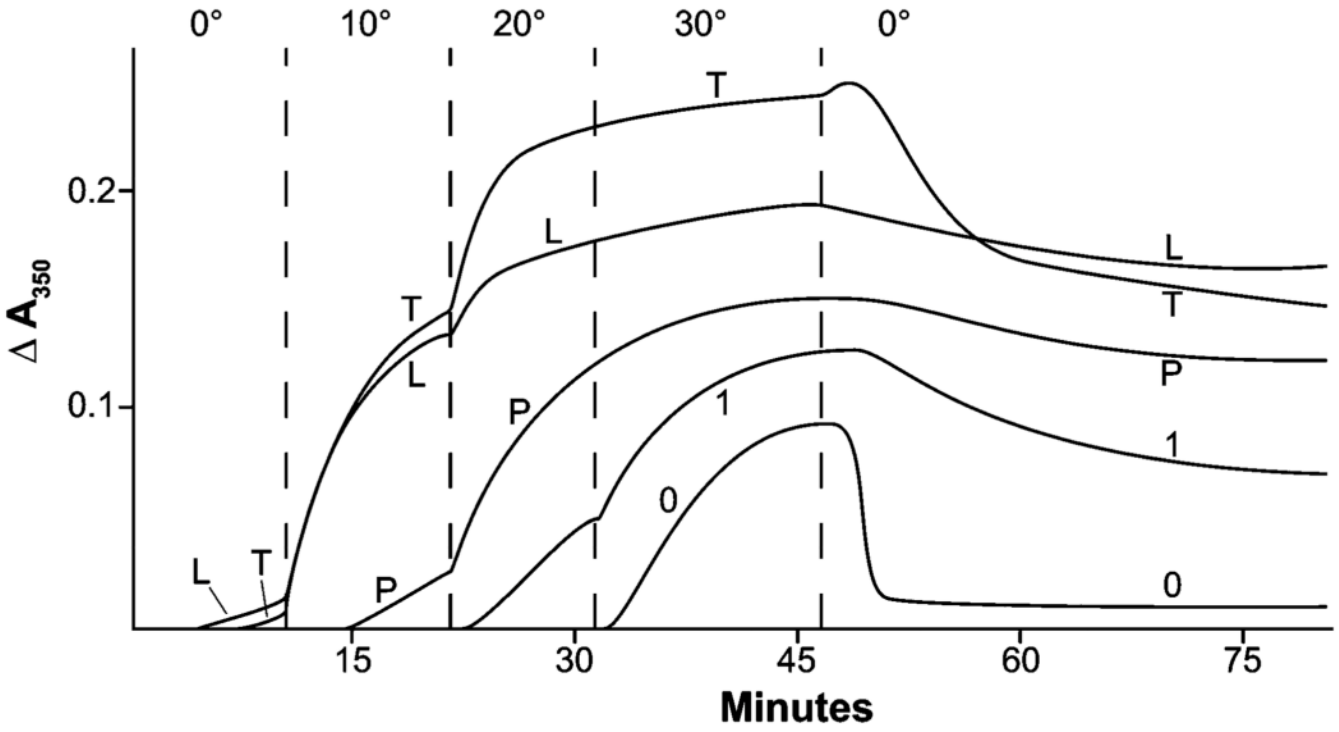

Figure 2.

Comparison of the effects of laulimalide, paclitaxel, peloruside A, and (11-*R*)-peloruside A on tubulin assembly. Each 0.25 mL reaction mixture contained 0.1 M 4-morpholineethane-sulfonate (1.0 M stock solution adjusted to pH 6.9 with NaOH), 0.1 mM guanosine 5′-triphosphate (GTP), 4% (v/v) dimethyl sulfoxide, 1.0 mg/mL (10 μM) tubulin, 0.75 mg/mL heat-treated microtubule-associated proteins, and the following compounds at 10 μM: curve 0, none; curve 1, 10 μM (11-*R*)-peloruside A; curve P, 10 μM peloruside A; curve T, 10 μM paclitaxel; and curve L, 10 μM laulimalide. The cuvette contents were initially at 0 °C for about 10 min. Subsequently, at the times indicated by the vertical dashed lines to the left of the temperatures shown, the temperature controller was set to the indicated temperature.

NIH-PA Author Manuscript

NIH-PA Author Manuscript

NIH-PA Author Manuscript

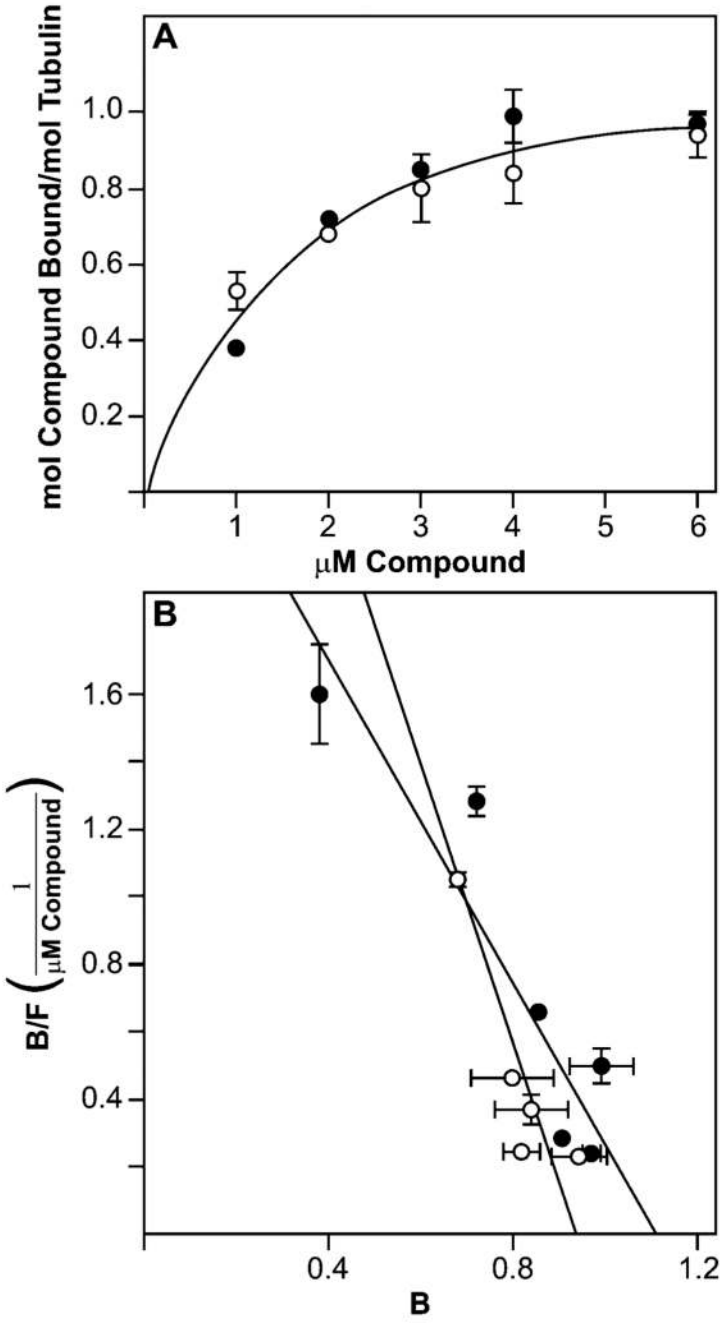

Figure 3.

Comparison of the binding of [^{3}H]peloruside A (solid symbols) and of [^{3}H]paclitaxel (open symbols) at different concentrations (A), with analysis of the data by the Scatchard method (B). Reaction mixtures were prepared and analyzed as described in the text and contained the indicated concentrations of the radiolabeled ligands. It should be noted that with 1.0 μM [^{3}H]paclitaxel, the data indicated total binding of compound in the reaction mixture to the microtubules. This point was therefore excluded from the Scatchard analysis, since it would not yield meaningful data (i.e., free drug = 0). Standard errors are shown, unless smaller than the symbol.

NIH-PA Author Manuscript

NIH-PA Author Manuscript

NIH-PA Author Manuscript

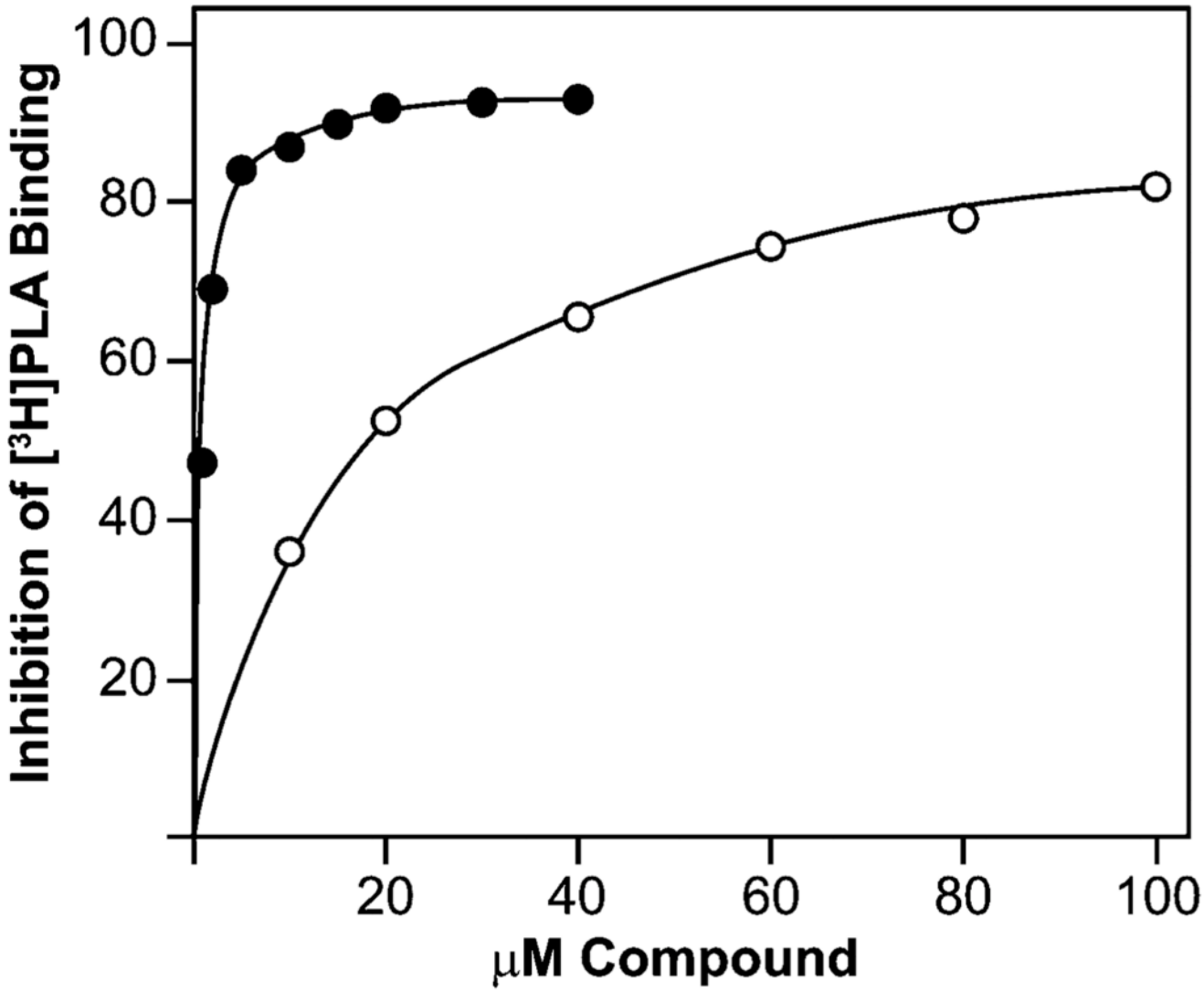

Figure 4.
Comparison of laulimalide (closed symbols) and (11-*R*)-peloruside A (open symbols) as inhibitors of the binding of [^{3}H]peloruside A to tubulin. Reaction mixtures were prepared and analyzed as described in the text.

NIH-PA Author Manuscript

NIH-PA Author Manuscript

NIH-PA Author Manuscript

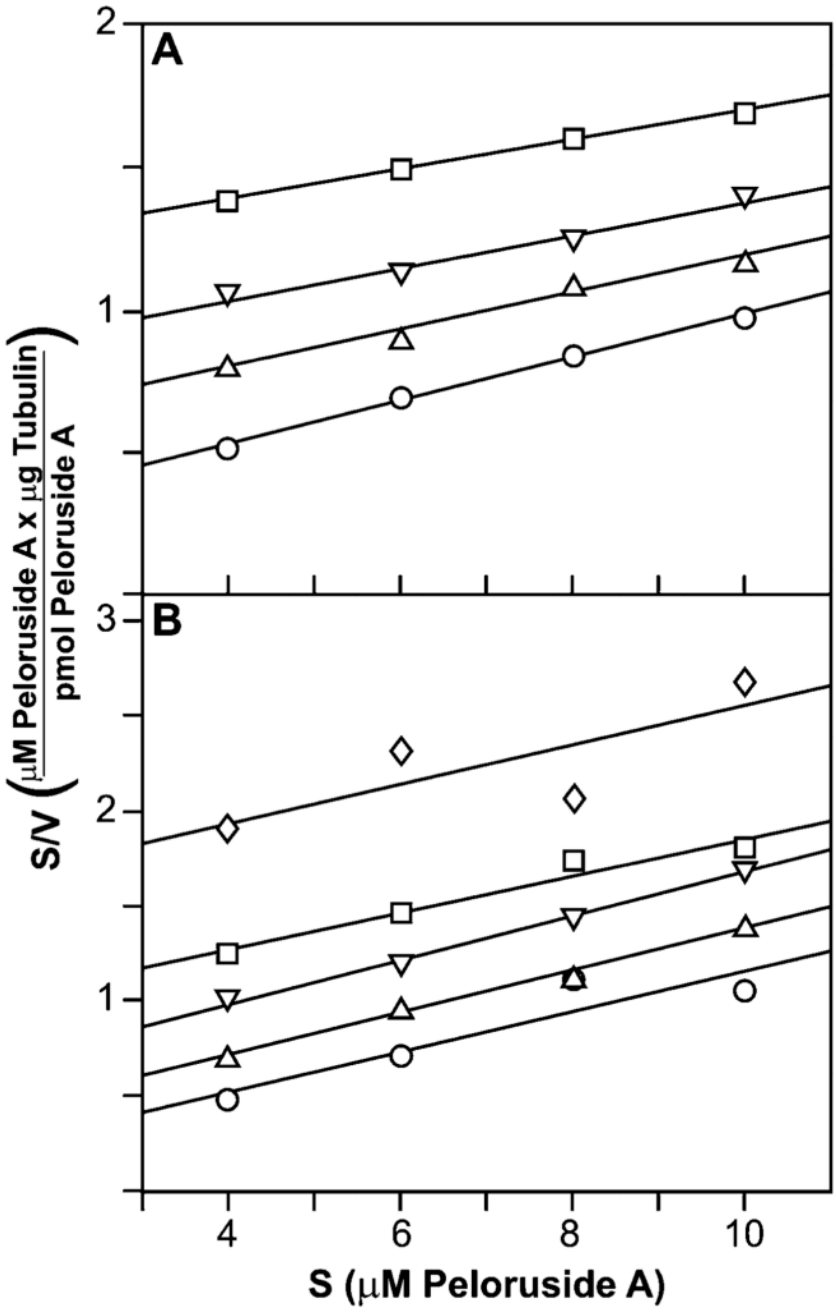

Figure 5.

Both (11-*R*)-peloruside A (A) and laulimalide (B) are competitive inhibitors of the binding of [^{3}H]peloruside A to microtubules as determined by Hanes analysis. Reaction mixtures were prepared and analyzed as described in the text. Samples contained the indicated concentrations of [^{3}H]peloruside A. (A) Concentrations of (11-*R*)-peloruside A were as follows: circles, none; upright triangles, 5.0 μM; inverted triangles, 10 μM; and squares, 20 μM. (B) Concentrations of laulimalide were as follows: circles, none; upright triangles, 0.5 μM; inverted triangles, 1.0 μM; squares, 1.5 μM; and diamonds, 2.0 μM.

NIH-PA Author Manuscript

NIH-PA Author Manuscript

NIH-PA Author Manuscript

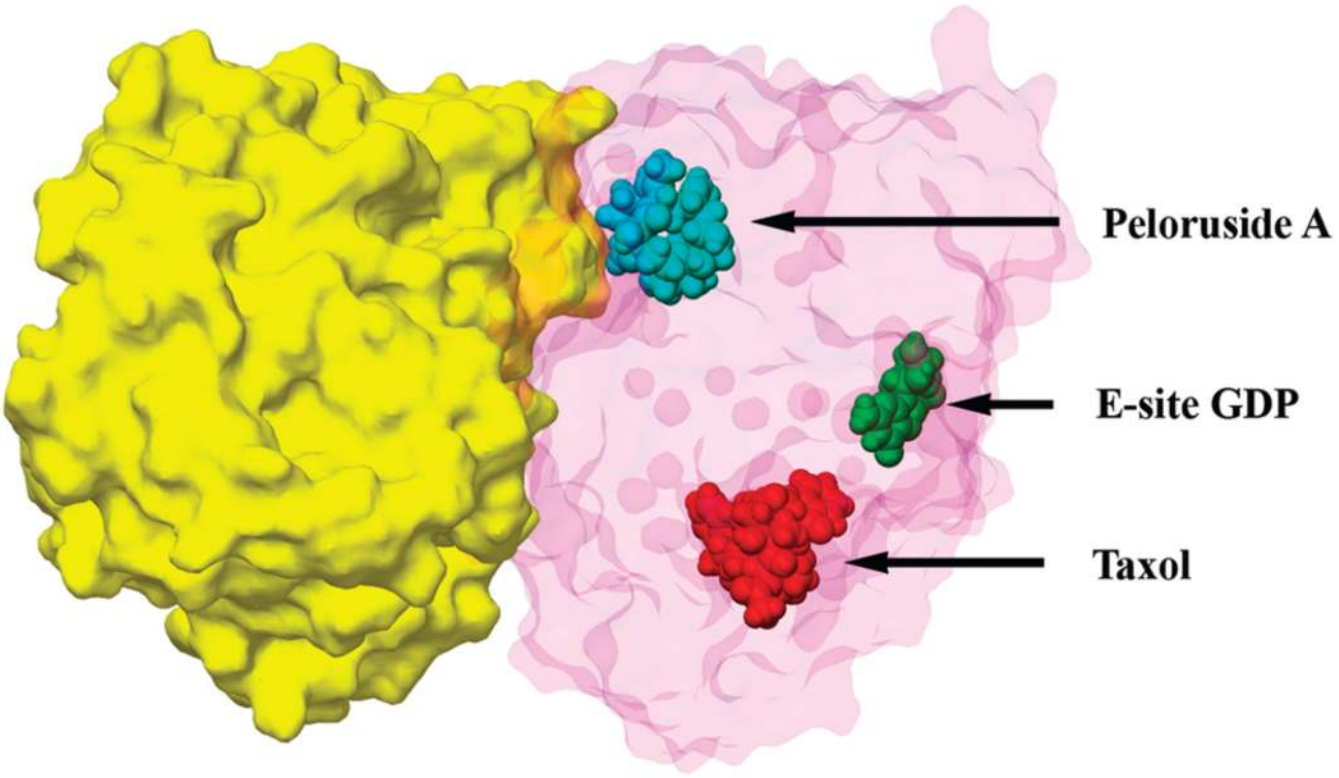

Figure 6.
Overview of the peloruside A binding site on β-tubulin, showing its position relative to the taxoid site and the exchangeable nucleotide site (E-site). The tubulin subunits are rendered as contoured surfaces, with α-tubulin colored yellow and β-tubulin colored transparent purple. Peloruside A, GDP, and paclitaxel are drawn in CPK and colored cyan, green, and red, respectively.

NIH-PA Author Manuscript
NIH-PA Author Manuscript
NIH-PA Author Manuscript

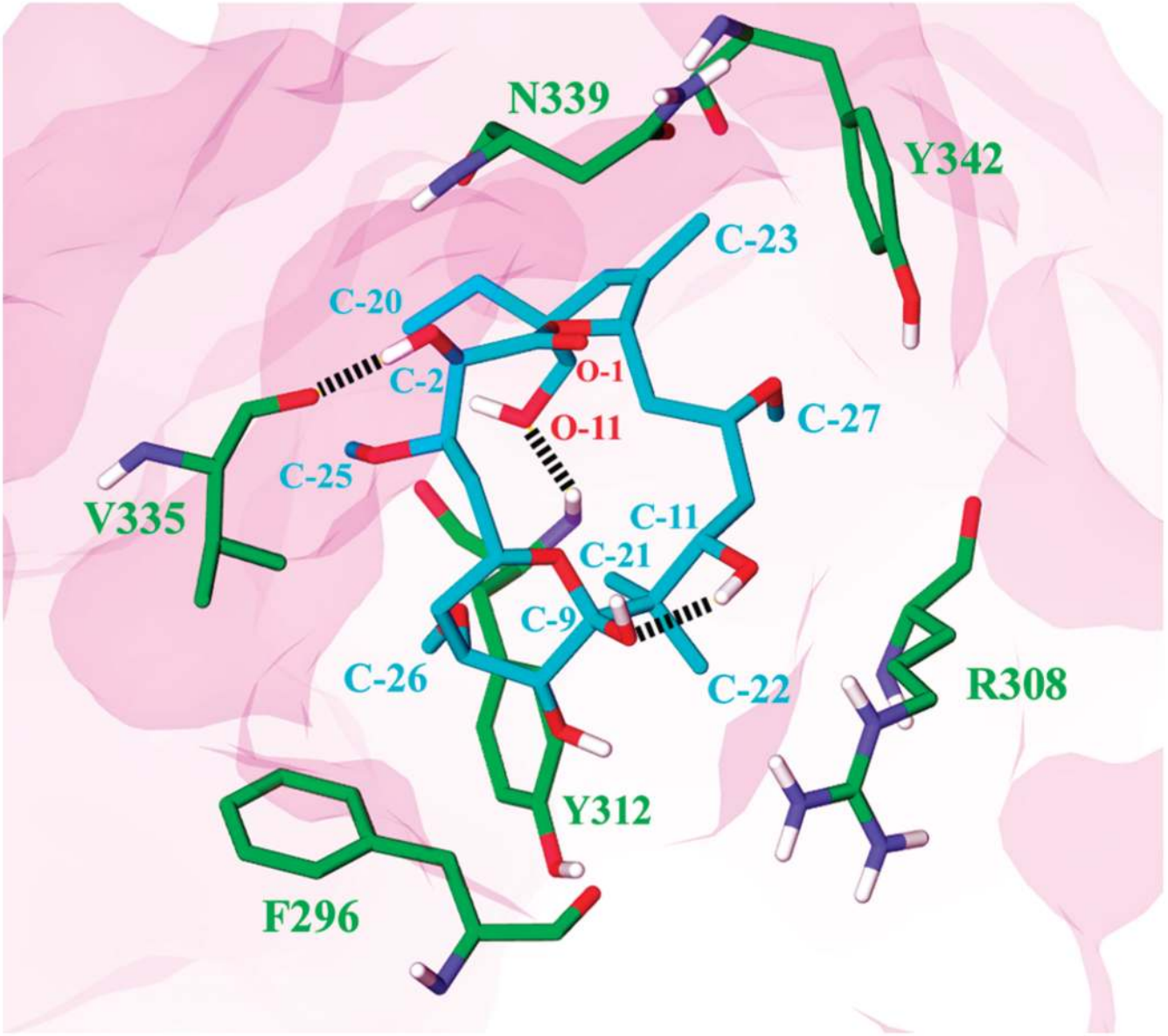

Figure 7.

Detailed pose of peloruside A bound to β-tubulin, highlighting the binding interactions. Peloruside A and the specific amino acid residues with which it interacts (see text) are shown as stick diagrams, with polar hydrogen atoms colored white and oxygen and nitrogen atoms colored red and blue, respectively. The carbon atoms of peloruside A and the amino acid residues are colored cyan and green, respectively. Hydrogen bonds are represented by dashed black lines. To illustrate the contours of the binding pocket, β-tubulin is rendered as a transparent purple surface.

NIH-PA Author Manuscript
NIH-PA Author Manuscript
NIH-PA Author Manuscript

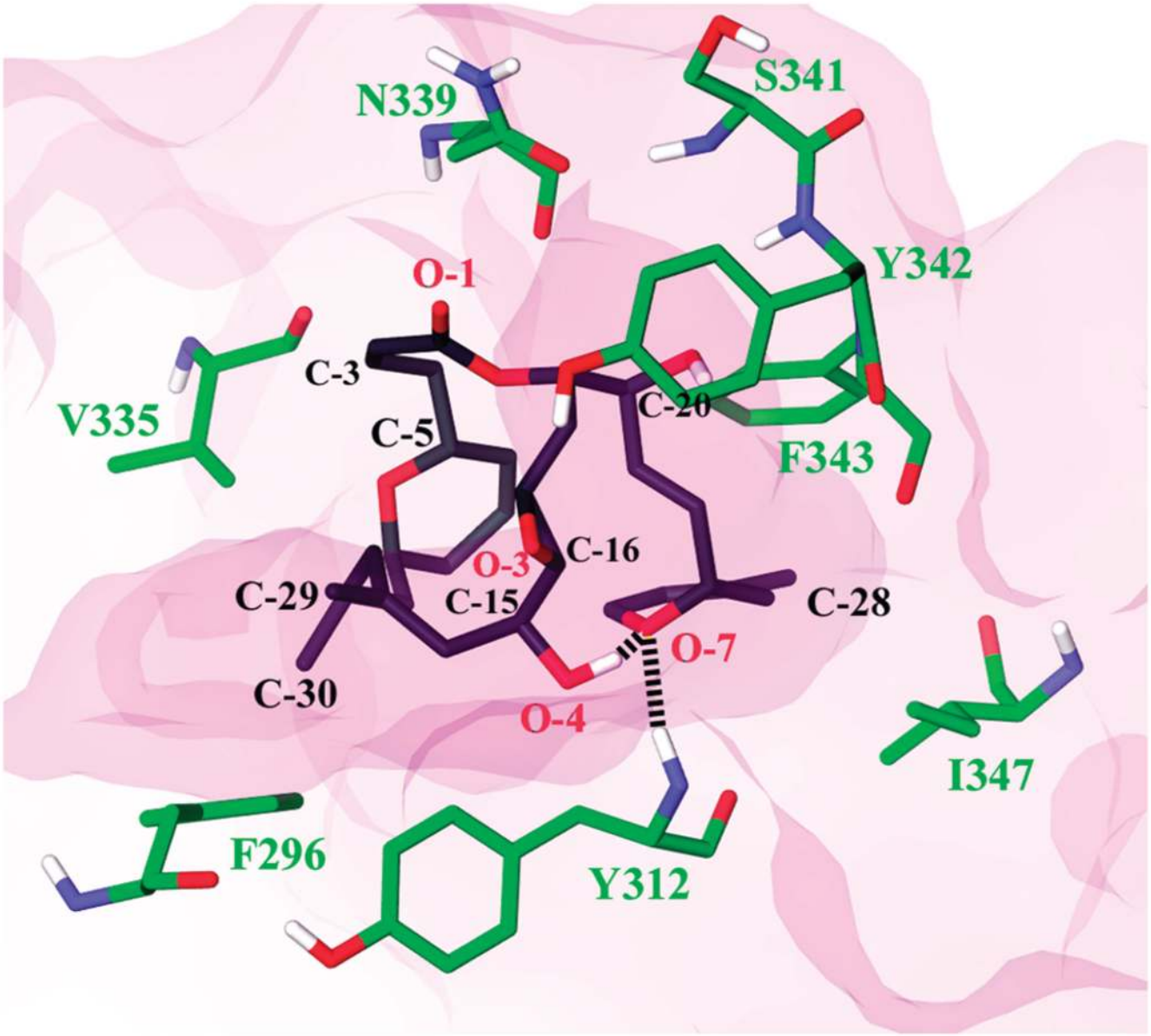

Figure 8.

Detailed pose of laulimalide bound to β-tubulin, highlighting the binding interactions. Laulimalide and the specific amino acid residues with which it interacts (see text) are shown as stick diagrams, with polar hydrogen atoms colored white and oxygen and nitrogen atoms colored red and blue, respectively. The carbon atoms of laulimalide and the amino acid residues are colored black and green, respectively. Hydrogen bonds are represented by dashed black lines. To illustrate the contours of the binding pocket, β-tubulin is rendered as a transparent purple surface.

NIH-PA Author Manuscript

NIH-PA Author Manuscript

NIH-PA Author Manuscript

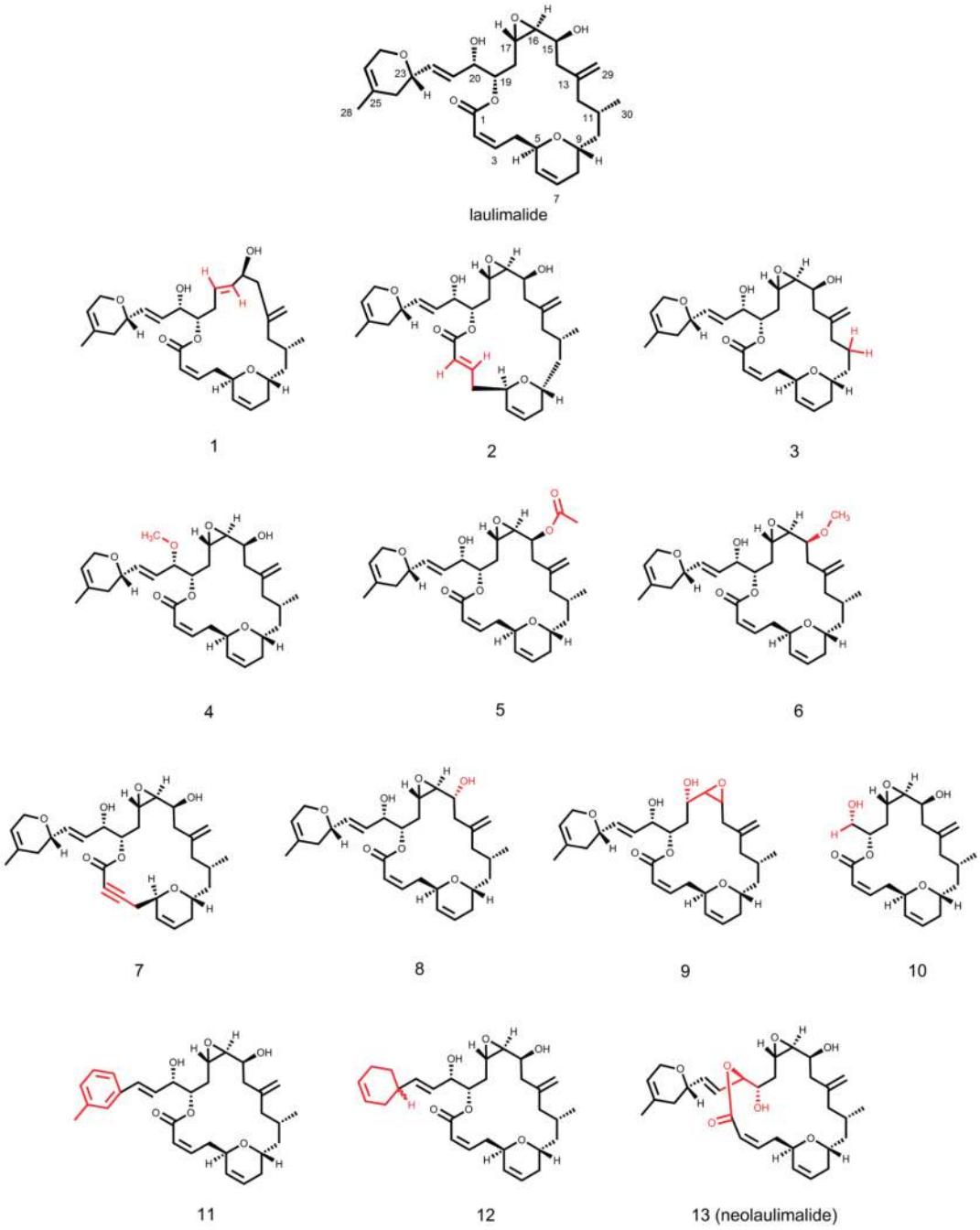

Figure 9.
Selected laulimalide analogues, to illustrate the structure–activity relationship description (see text). Differences from the laulimalide structure are indicated in red.

NIH-PA Author Manuscript
NIH-PA Author Manuscript
NIH-PA Author Manuscript

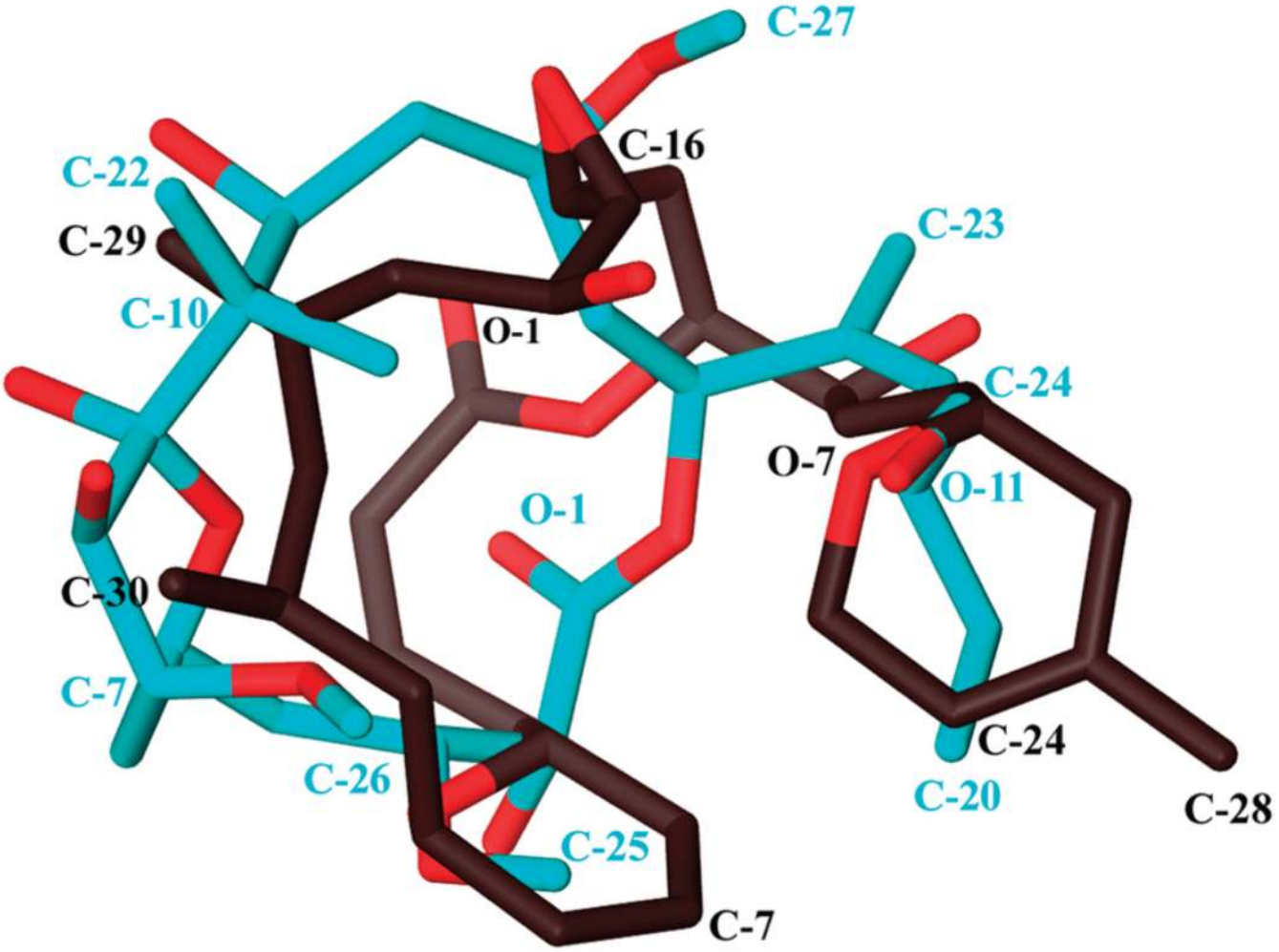

Figure 10.
Superimposition of the bound conformations of peloruside A and laulimalide as they fit into the binding pocket. Structures are rendered in stick, with oxygen atoms colored red. The carbon atoms and position labels for peloruside A and laulimalide are colored cyan and black, respectively.

NIH-PA Author Manuscript

NIH-PA Author Manuscript

NIH-PA Author Manuscript

Table 1

Inhibition of [^{3}H]Peloruside A and [^{3}H]Paclitaxel Binding to Microtubules[a]

	% inhibition ± SD	
	radiolabeled ligand	
potential inhibitor	[^{3}H]peloruside A	[^{3}H]paclitaxel
laulimalide	90 ± 0.1	1.7 ± 5
(11-*R*)-peloruside A	49 ± 1	0 ± 8
peloruside A		5.1 ± 6
paclitaxel	6.8 ± 0.5	
epothilone B	2.2 ± 5	79 ± 5
discodermolide	5.0 ± 2	87 ± 2

[a]Reaction mixtures contained the components described in the text, including 2.0 μM tubulin polymerized into microtubules, the radiolabeled ligand at 4.0 μM, and the potential inhibitors at 20 μM. Incubation and centrifugation as described in the text.